

RBF Neural Network for Landmine Detection in Hyperspectral Imaging

Original

RBF Neural Network for Landmine Detection in Hyperspectral Imaging / Makki, Ihab; Younes, Rafic; Khodor, Mahdi; Khoder, Jihan; Francis, Clovis; Bianchi, Tiziano; Rizk, Patrick; Zucchetti, Massimo. - ELETTRONICO. - (2018), pp. 1-6. (Intervento presentato al convegno 2018 7th European Workshop on Visual Information Processing (EUVIP) tenutosi a Tampere, Finland nel 26-28 Nov. 2018) [10.1109/EUVIP.2018.8611652].

Availability:

This version is available at: 11583/2724277 since: 2019-01-31T15:44:15Z

Publisher:

IEEE

Published

DOI:10.1109/EUVIP.2018.8611652

Terms of use:

This article is made available under terms and conditions as specified in the corresponding bibliographic description in the repository

Publisher copyright

IEEE postprint/Author's Accepted Manuscript

©2018 IEEE. Personal use of this material is permitted. Permission from IEEE must be obtained for all other uses, in any current or future media, including reprinting/republishing this material for advertising or promotional purposes, creating new collecting works, for resale or lists, or reuse of any copyrighted component of this work in other works.

(Article begins on next page)

RBF Neural Network For Landmine Detection In Hyperspectral Imaging

Ihab Makki

Faculty of Engineering

Lebanese University

Beirut, Lebanon

ihab.makki@polito.it

Jihan Khoder

Faculty of Engineering

Lebanese University

Beirut, Lebanon

jihan.khoder@hotmail.com

Patrick Rizk

Université du Québec à Rimouski

Québec, Canada

patrickrk17@gmail.com

Rafic Younes

Faculty of Engineering

Lebanese University

Beirut ,Lebanon

ryounes@ul.edu.lb

Clovis Francis

Faculty of Engineering

Lebanese University

Beirut ,Lebanon

cfrancis@ul.edu.lb

Mahdi Khoder

Politecnico di Torino

Torino,Italy

mahdi.khoder89@gmail.com

Tiziano Bianchi

Politecnico di Torino

Torino,Italy

tiziano.bianchi@polito.it

Massimo Zucchetti

Politecnico di Torino

Torino, Italy

massimo.zucchetti@polito.it

In this work, we evaluate different classification algorithms used for multi-target detection in hyperspectral imaging. We took into consideration the scenario of landmine detection in which we compared the performance of each method in various cases. In addition, we introduced the detection of targets using artificial intelligence-based methods in order to obtain better detection performance together with target identification and estimation of its abundance. These algorithms were tested on various types of hyperspectral images where the spectra of the landmines were planted in different proportions in the hyperspectral scenes. The results show the advantage of using our training strategy for radial basis function neural networks (RBFNN) in order to detect, identify and estimate the abundance of the targets in hyperspectral images at the same time. Moreover, the proposed technique requires a comparable computational cost with respect to state of art target detection techniques.

Keywords— Hyperspectral Imaging, RBF Neural Network, landmine detection, remote sensing.

I. INTRODUCTION

Hyperspectral imaging or imaging spectroscopy is a trending technique in remote sensing. It is widely used in different fields like agriculture [1], food quality monitoring [2], surveillance [3], target detection [4,5], and many others. Thanks to this technology, we are able to detect at each pixel, the portion of light reflected in hundreds of wavelengths. By this, we obtain a three-dimensional data structure that contains both spatial and spectral information: the first and second dimensions contain spatial information and the third one includes the spectral

information. Knowing the portion of light reflected at each wavelength, we get what we call the reflectance spectrum. This spectrum can be used as a fingerprint to identify the material at each pixel.

Due to the great impact of the problem of landmines on modern societies [6], we are focusing in our studies on the detection of landmines using hyperspectral imaging. This technique has the potential to reduce the time needed to detect landmines and at the same time to make the detection safer.

In this paper, we propose a supervised landmine detection algorithm based on a radial basis function neural network (RBFNN) built using a customized training strategy. In addition, we test different algorithms and image processing tools usually used for target or anomaly detection using hyperspectral imagery. The goal of this test is to evaluate and compare the performance of the proposed technique with state of art techniques in the detection of different types of landmines at the same time.

Several algorithms have been proposed for target detection in hyperspectral imagery [7,8]. Most of them do not support multitarget detection unless we run them several times each run for a specific target, like Spectral Angular Mapper (SAM), Adaptive Coherence Estimator (ACE), Matched Filter (MF) [9]. However, this will be a time-consuming process especially if the number of targets is high. Some algorithms were extended for multitarget case e.g. the Constrained Energy minimization (CEM) algorithm, originally made to give an estimation of the abundance of the target, has several extensions to fit the multi target detection scenario: multiCEM, SumCEM, Winner-take-all CEM (WTACEM) and others [10]. Other unsupervised

algorithms may be used to detect targets without referring to their reflectance spectrum [11].

In this paper, we propose a customized training strategy to train an RBFNN for the goal of multitarget detection using hyperspectral imagery. We will compare the performance of the proposed method in different types of images.

The paper is organized as follows: in Section 2 we introduce the RBFNN. In Sections 3 we describe our experimental setting while in Section 4, we evaluate the performance of the proposed method by comparison with existing methods when applied on images with planted targets simulating the landmine detection scenario. Discussion and conclusions are drawn in Section 5 and Section 6, respectively.

II. NEURAL NETWORKS BASED TARGET DETECTION

In this section, we will introduce the use of artificial intelligence in order to detect targets in hyperspectral imagery. Specifically, we will work on neural networks (NN).

Artificial Neural Network (ANN) is a computational model used for various machine learning and computer vision tasks. It is designed to work in the same way as the neural networks of the human brain [12]. It is composed of network of connected units called “neurons” where each connection has a weight. The neurons are grouped into layers. In addition to the weights, each layer has a bias that plays a crucial role in the detection [13]. A basic NN is composed of two layers: input layer and output layer. This type of NN is called Single layer NN. Other type of NN may have additional hidden layers between the input and output layers. In this category, we can find the Multi-Layer Perceptron (MLP). This kind of ANN has the ability to solve nonlinear complex problems that the single layer NN will not be able to solve [13].

Another type of neural networks is the Radial basis functions neural network. It has the same structure of layers as the MLP. However, in the hidden layer, the activation function is a kernel function (usually Gaussian) [14]. Usually, MLP NN are faster than RBF NN as their computation do not necessitate the use of kernels and is therefore simpler. However, in case of high dimensional data, as in our case where the pixel is of 189 bands dimensions, the RBF performs better. RBF showed better

performance in our case and thus we will adopt this method in the comparison.

Here, we used a two-layers RBF neural network (Fig.1). The activation function of the first layer (hidden layer) is a Gaussian kernel defined as

$$Z(x) = \frac{\exp(-\|x - \mu\|^2)}{\sigma^2}$$

where μ is an n-dimensional vector called the center of the radial basis function and σ is a width parameter related to the spread of the function around its center.

In our hyperspectral image case, the training set is composed of group of signatures classified between landmines and background material. Each input is a signature of a material introduced as a vector. So the number of neurons in the input layer is equal to the number of bands used in the test. The number of neurons in the output layer is equal to the number of targets plus one to represent each target class plus the background class. In the hidden layer, the number of neurons, which equal the number of centers μ , is empirically estimated to minimize the global problem. The centers are randomly chosen from a subset of the training dataset. The spread parameter is calculated in such a way as to achieve a certain amount of overlapping between neighbor radial basis functions to form a smooth and contiguous interpolation of the input space [26].

The weights are first randomly set and then they are updated during the training phase using the gradient decent rule [27]. The activation function of the output layer is linear.

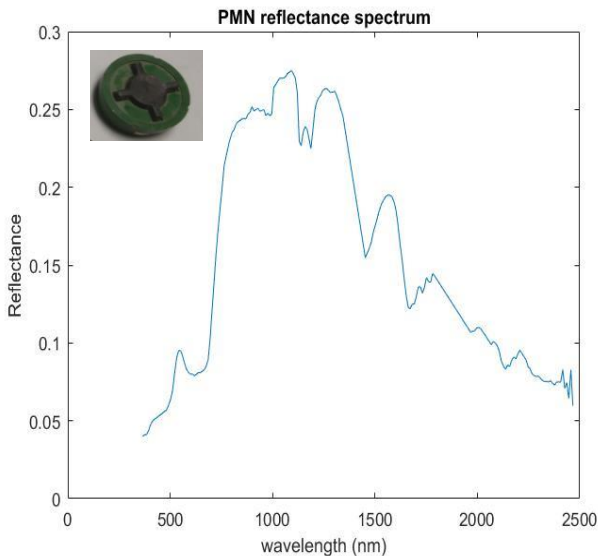
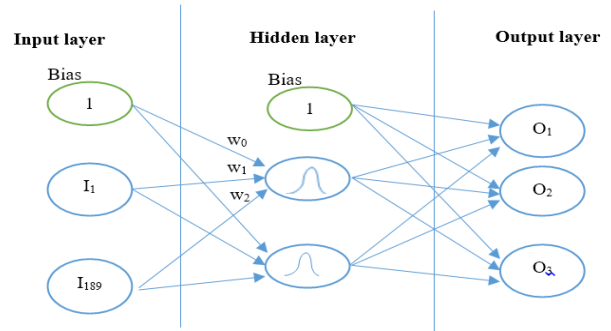


Fig 2: Reflectance spectrum of the pmn mine (target) inserted in the image

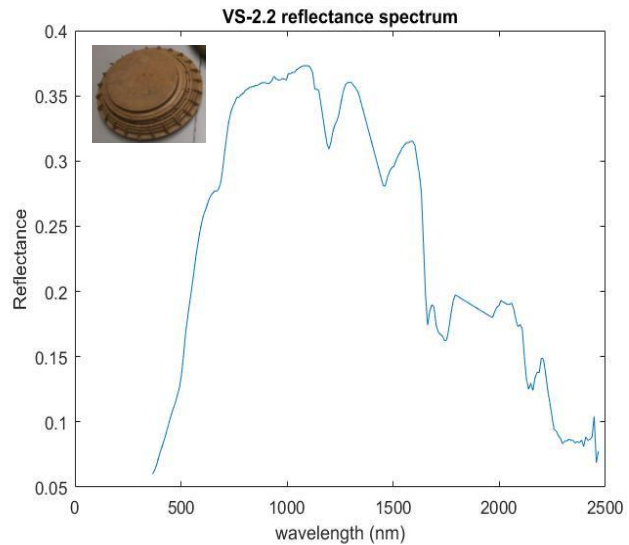


Fig.3: Reflectance spectrum of the vs-2.2 mine (target) inserted in the image

Fig. 1: Architecture of the RBFNN used in this test

III. COMPARATIVE STUDY

We tested the target detection algorithms on 17 hyperspectral images taken using Airborne Visible/Infrared Imaging Spectrometer (AVIRIS) of JPL NASA Laboratory. These scenes are available online on the site [15]. This airborne sensor detects hyperspectral images between 394nm and 2500nm with spectral resolution of 10nm in 224 bands. The spatial resolution of the images depends on the altitude of the airplane during image acquisition. We can find different scenes of different spatial resolutions. To limit the effect of noise, we discarded some bands characterized by low Signal to Noise Ratio (SNR) due to water vapor absorption effect. For this reason, we are going to use 189 out of 224 bands. In the chosen scenes, we introduced in different locations the spectrum of two types of landmines: the PMN anti-personnel landmine (Fig.2) and VS-2.2 anti-tank mine (Fig.3). The reflectance spectra of the landmines were taken in our Lab using Field Spec 4 Hi-Res spectroradiometer. This device is able to acquire the reflectance spectrum between 350 and 2500 nm with spectral resolution of 1nm. We took the spectral signature in different conditions: in a laboratory using a specific source of light, and by deploying the landmine cases in either a grass field or bare soil during a sunny day. In our experiments, we implant in the AVIRIS scenes the spectral reflectance taken when thin layers of grass covered the landmine, as grass is the dominant background material in the used scenes. We admitted the target implant method in this case because we are simulating the landmine detection scenario where it is very hard and dangerous to acquire hyperspectral data of real minefields and such images are not available on public datasets. In addition, it has been proven in [28] that the target implant method does provide accurate relative predictions in terms of both target difficulty and detector performance.

The insertion was done after several image-preprocessing steps: firstly, atmospheric correction is done to convert the image from radiance domain that depends on the illumination and weather conditions into unified reflectance domain scaled between 0 and 1. Then the image is upsampled in order to increase the spatial resolution of the image to arrive to pixel size equivalent to the size of the mine. Some bands characterized by low SNR due to vapor absorption are discarded. As the spectra spectrum of the mine is very high, we took the reflectance of the mines in the bands that match the bands of the image.

In order to test the full pixel and subpixel cases, the targets were planted in different proportions in the images. The signatures of the landmines were mixed with the neighboring pixel signature in different fill fractions using the following formula:

$$PS = \alpha * T + (1 - \alpha) * B$$

where PS represents the planted spectrum in the image, T is a vector containing the target reflectance spectrum, B is the reflectance spectrum of the background material and α is the target fill fraction which is in other terms the abundance of the target in the planted pixel. In our experiments, we considered

values of α varying between 0.6 and 0.9. Different values of abundance factor α are used to minimize the contrast between the implanted pixel and its surrounding making the detection harder. In the 17 images, the total number of pixels with landmine abundance factor of $\alpha = 0.6$ (PMN& VS-2.2) is 136, 170 have landmine abundance factor $\alpha = 0.7$, 102 have landmine abundance factor $\alpha = 0.8$ and 110 pixels have landmine abundance factor $\alpha = 0.9$.

IV. RESULTS

In this section, we show a comparative study between several target detection algorithms in order to evaluate performance based on three metrics:

- Probability of detection (Pd) which is the number of detected targets over the number of actual targets in the scene.
- False Alarm rate (FAR), which represents the number of false positives (i.e., pixels marked as targets while they are not). To normalize between different images, the false alarm is computed per unit area (e.g per square meter.)
- Computation Time (CT) which represent the CPU time in seconds needed to compute the algorithms.

The tested algorithms used in this paper are: Spectral Angular Mapper (SAM) [20], Orthogonal Subspace Projection (OSP) [21], Adaptive Coherence Estimation (ACE) [22], Constrained Energy Minimization (CEM) [23], Multiple target CEM (MTCEM) [23], Winner take all CEM (WTACEM), Sum CEM (SCEM)[23], Spectral Information Divergence (SID) [23], Matched Filter(MF) [23] and the proposed radial basis function neural network (RBFNN).

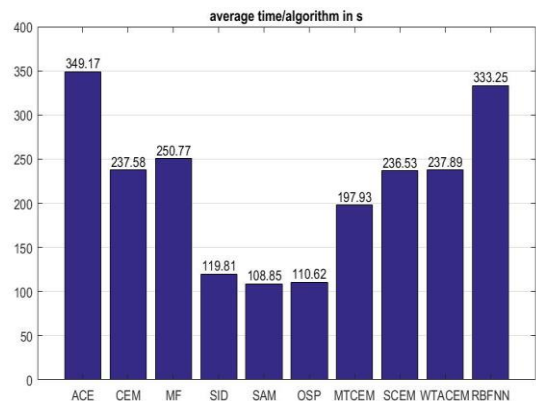


Fig. 4: Average computational time /algorithm

To compare the results, we may use the Receiver Operating Curve (ROC), which is the plot of Probability of Detection versus the FAR. However, in our case, ROC is not very useful due to the rarity of targets. For this reason, we adopted the following comparison strategy:

Each time we apply a target detection algorithm, we get a value between zero and one that represents the degree of similarity

between the pixel and the target. The presence or the absence of the target is decided according to a threshold affecting the Pd and FAR registered by each method. For this reason, to be able to compare between different algorithms, the decision threshold used to discriminate between target and background material is set to be the lowest value such that all targets are detected (Pd=1) and then the FAR is registered. Therefore, a technique is said to be more efficient if it has lower FAR when all targets have been detected.

In the case of neural networks, the best NN that gives a Pd=1 with minimum FAR was individuated after several tests where we took into consideration different training samples and spread values. First, we randomly divided the 17 images between training and testing data where we used some images in order to train the NN and the other images to evaluate the performance. Using this strategy, the training was very intensive process, took a long time, necessitating a large number of neurons to consider all possible cases and we did not arrive to zero FAR. In order to make the training process less intensive and to avoid the problem of overfitting the network, we found that training the network using only few pixels that represent the image endmembers is sufficient to obtain a NN able to estimate the abundance of targets and background in each pixel. Therefore, in the training phase, an estimation of the endmembers of the images (an estimation of basic materials that are composing the scenes) in addition to the spectra of the landmines are used. The spectra of the endmembers are estimated using Automatic Target Generation Process (ATGP) algorithm [16] which gives estimation signatures for each endmember. It is not necessary that these signatures exist literally in the image, because each pixel of the image may be made of a linear combination of different endmembers.

The input training dataset is formed of 377 background spectra, 5 spectra of PMN mine and 5 spectra of VS-2.2 mine. The corresponding outputs are respectively [0,0,1],[1,0,0], and [0,1,0]. Since the network is trained with the pure reflectance spectrum of the target, by using this training strategy the output for each pixel will be a vector estimating the abundance fraction of PMN, VS-2.2, or general background. As the minimum fill fraction of the landmines is 0.6, we set a fixed threshold =0.5 for the first two entries of the output vector. If the first entry of the output is higher than 0.5, the pixel is considered a PMN mine. If the second entry is higher than 0.5, the pixel is marked as VS-2.2 landmine. Otherwise, the pixel is marked as background. An example of the output of the proposed network is shown in Fig. 6. The key strength of our approach is that with relatively small training set composed of 387 spectra, we were able to detect, classify and estimate the abundance of the landmines in 17 images, where each image has more than 600000 pixels.

In Figure 4, we show the average time needed per each algorithm to detect all the targets in the 17 images. As we see in the figure, ACE, CEM, MF MTCEM, SCEM, WTACEM and RBF-NN take high computational time to detect the two types of mines by comparison with SAM OSP and SID that have a lower computation time.

Regarding the FAR (Figure 5), we see that almost all algorithms could detect the targets with very low FAR except for SID and SAM that have high FAR.

The other algorithms show very good performance even in case of small abundance factor where few FA shows up when trying to detect low abundance targets using MF and CEM. ACE algorithm gives the ability to detect all targets with 0 FAR. This confirms the previous tests used for target detection [8,17].

On the other hand, MTCEM has better performance as all targets are detected without any false alarms with lower computation time. It should be pointed out that, using ACE MF CEM SID SAM and OSP; we have an additional advantage when identifying the targets since using these algorithms we are able to distinguish between PMN and VS-2.2 targets. While using the other algorithms, we can know the presence of a target without knowing its type. An additional similarity test is needed in case of MTCEM, WTACEM and SCEM to be able to estimate the type of the landmine that exist in this position. However, the abundance of the landmine is still unknown by using the similarity test.

As we see in the charts, using the adopted training strategy, we got an RBF NN able to detect the landmines without any false alarm. By setting a large value of spread (σ) while training the NN, the output was less sensitive to the spectral variability of the input pixel and able to distinguish the presence of target even with low abundance factor.

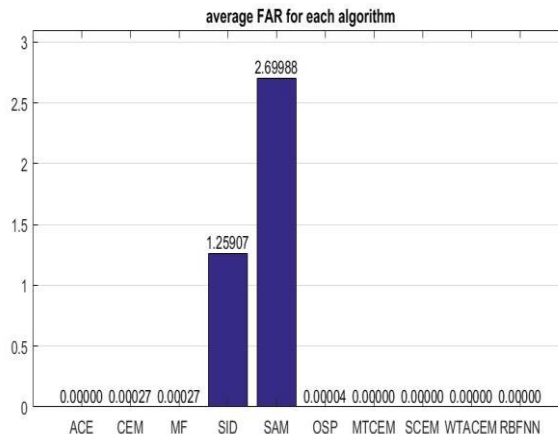


Fig.5: average FAR/ algorithm

V. DISCUSSION

In this experiment, we tested some supervised multitarget detection algorithms using hyperspectral imagery. We tested simulated data where the reflectance spectrum of the target was planted in the scene in different places. Some of the tested algorithms (ACE, MF, CEM, OSP, SAM, SID) are designed for the detection of one target. They were applied several times each run for each target. This may be a time-consuming process, especially if the number of targets is high. This is why we addressed the multitarget detection in this paper. When using some of the multitarget detection process, we lose the privilege of identifying the type of the target. However, this can be recovered by an additional similarity test to classify each target.

SAM and SID are similarity measures between pixel signatures and target reflectance spectrum. The former calculates the angle between the target spectrum and the pixel spectrum, while the latter calculates the entropy between them. When the pixel spectrum is a linear mixture of target and other background material, the similarity measure will differ according to the abundance fraction of the target making the detection process harder. This is the reason of the high false alarm rate that appeared in the tests.

Using RBF-NN, we are able to detect, identify the targets and to estimate the abundance fraction without any problem. The proposed strategy for training an RBF NN has reduced the size of the used NN making also possible to estimate the abundance fraction of the targets. In the test shown in this paper, we got a full detection rate without any false alarm rate. This may be due to the following reasons: by using a kernel function in the hidden layer, we are projecting the data into higher dimensional space where the classification of the target is simpler. In addition, by using a high spread value, we are adapting the NN to detect the signature of the target even if the implanted signature was modified when mixed with background pixels. Therefore, we were able to detect targets at the subpixel level. The results proves the advantage of using NN for target detection in the proposed landmine detection scenario.



Fig. 6 : A sample of the output of the RBF when applied on one image. White circles represents the location of the inserted PMN mines in the image, yellow circles are the placement of the VS-2.2 mine.

VI. CONCLUSION

In this paper, we addressed the problem of multitarget detection using hyperspectral imaging technique. Several methods already exist in the literature, like MTCM SCM and WTACEM, that have been designed to achieve this purpose. However, when using these techniques, we lose a key information about the type of the target. This information is

crucial in many target detection fields especially in mine detection where the knowledge of the type of the mine is necessary to manage the demining process accordingly.

When using RBFNN, not only we are able to detect targets without any false alarm, but we are also able to identify the type of the target and, at the same time, estimate its abundance. This is a great improvement in this domain since the abundance fraction data may give an idea about how deep the mine is buried in the soil and help to better recognize it.

In future work, the computational time of this method may be optimized by addressing the dimensionality reduction [19] and data preservation methods [18] before target detection, in order to achieve real time detection during image acquisition.

VII. REFERENCE

- [1] Vigneau, Nathalie, Martin Ecarnot, Gilles Rabatel, and Pierre Roumet. "Potential of field hyperspectral imaging as a non destructive method to assess leaf nitrogen content in Wheat." *Field Crops Research* 122, no. 1 (2011): 25-31.
- [2] Gowen, A. A., CPo O'Donnell, P. J. Cullen, G. Downey, and J. M. Frias. "Hyperspectral imaging—an emerging process analytical tool for food quality and safety control." *Trends in Food Science & Technology* 18, no. 12 (2007): 590-598.
- [3] Yuen, P. WT, and Mark Richardson. "An introduction to hyperspectral imaging and its application for security, surveillance and target acquisition." *The Imaging Science Journal* 58, no. 5 (2010): 241-253.
- [4] Chang, Chein-I. *Hyperspectral imaging: techniques for spectral detection and classification*. Vol. 1. Springer Science & Business Media, 2003.
- [5] Makki, Ihab, Rafic Younes, Clovis Francis, Tiziano Bianchi, and Massimo Zucchetti. "A survey of landmine detection using hyperspectral imaging." *ISPRS Journal of Photogrammetry and Remote Sensing* 124 (2017): 40-53
- [6] M. Zucetti, M. Khoder, I. Makki, R. Younes, C. Francis, T. Bianchi "Landmines.Crisis, legacy, international and local action". 2017 First International Conference on, pp. 1-3. IEEE, 2017.
- [7] Manolakis, Dimitris, and Gary Shaw. "Detection algorithms for hyperspectral imaging applications." *IEEE signal processing magazine* 19, no. 1 (2002): 29-43.
- [8] Ihab Makki, Rafic Younes, Clovis Francis, Tiziano Bianchi, and Massimo Zucchetti. "Classification algorithms for landmine detection using hyperspectral imaging." In *Landmine: Detection, Clearance and Legislations (LDCL)*, 2017 First International Conference on, pp. 1-6. IEEE, 2017.
- [9] Du, Q., Ren, H., & Chang, C.-I. (2003). A Comparative Study for Orthogonal Subspace Projection and Constrained Energy Minimization. *IEEE Transactions On Geoscience And Remote Sensing*, 1525-1529.
- [10] Yin, Jihao, Yan Wang, Yisong Wang, and Zhanjie Zhao. "A modified algorithm for multi-target detection in hyperspectral image." In *Informatics in Control, Automation and Robotics (CAR)*, 2010 2nd International Asia Conference on, vol. 3, pp. 105-108. IEEE, 2010.
- [11] Plaza, Antonio, Pablo Martínez, Rosa Pérez, and Javier Plaza. "A new method for target detection in hyperspectral imagery based on extended morphological profiles." In *Geoscience and Remote Sensing Symposium*, 2003. IGARSS'03. Proceedings. 2003 IEEE International, vol. 6, pp. 3772-3774. IEEE, 2003.
- [12] McCulloch, Warren; Walter Pitts (1943). "A Logical Calculus of Ideas Immanent in Nervous Activity". *Bulletin of Mathematical Biophysics*. 5 (4): 115–133. doi:10.1007/BF02478259
- [13] Bishop, Christopher M. *Pattern recognition and machine learning*. springer, 2006 p228
- [14] Wu, Yue, Hui Wang, Biaobiao Zhang, and K-L. Du. "Using radial basis function networks for function approximation and classification." *ISRN Applied Mathematics* 2012 (2012).
- [15] <http://aviris.jpl.nasa.gov>

- [16] H. Ren and C.-I. Chang, "Automatic spectral target recognition in hyperspectral imagery," *IEEE Transactions on Aerospace and Electronic Systems*, vol. 39, no. 4, pp. 1232–1249, October 2003.
- [17] Manolakis, Dimitris, Ronald Lockwood, Thomas Cooley, and John Jacobson. "Is there a best hyperspectral detection algorithm?." In *SPIE Defense, Security, and Sensing*, pp. 733402-733402. International Society for Optics and Photonics, 2009
- [18] J. Khoder, R. Younes. "Proposal for Preservation Criteria to Rare Event. Application on Multispectral/Hyperspectral Images". 25th IEEE International Conference on Microelectronics (2013)
- [19] Khoder, Jihan, Rafic Younes, Hussein Obeid, and Mohamad Khalil. "Dimension reduction of hyperspectral image with rare event preserving." In *Iberian Conference on Pattern Recognition and Image Analysis*, pp. 621-629. Springer, Cham, 2015.
- [20] Osmar Abilio de carvalho Jr, Paulo Roberto Meneses, "spectral correlation Mapper(SCM):An improvement on the spectral Angle Mapper (SAM)", *summaries of the third annual JPL Airbone geoscience Workshop*, p 147-149, United state, 1992
- [21] Joseph C.Hatsanyi, Chein-I Chang, "Hyperspectral Image Classification and Dimensionality Reduction: An Orthogonal Subspace Projection Approach", *IEEE transaction on geoscience and Remote Sensing*, Vol 32, No 4, 1994
- [22] Shawn Kraut, Louis L.Scharf, Ronald W.Butler, "The Adaptive Coherence Estimator: A Uniformly Most-Powerful-Invariant Adaptive Detection Statistic", *IEEE Transaction on Signal Processing*, Vol 53, No 2, 2005
- [23] Camacho Velasco, César Augusto Vargas García, Henry Arguello Fuentes, "A comparative study of target detection algorithms in hyperspectral imagery applied to agricultural crops in Colombia", *Revista Tecnura*, Vol 20, No 49, 2016
- [24] Mahdi Khoder, Serge Kashana, Jihan Khoder, Rafic Younes, "Multicriteria classification method for dimensionality reduction adapted to hyperspectral images" *Journal of Applied Remote Sensing*, Vol 11, No 2, 2017
- [25] Jihan.Khoder, Rafic.Younes, "Dimensionality reduction on hyperspectral images: A comparative review based on artificial data" 4th International Congress on Image and Signal Processing, IEEE, 2011
- [26] Yousef, Rana, and Ke Hindi. "Training radial basis function networks using reduced sets as center points." *International Journal of Information Technology* 2, no. 1 (2005): 21-35.
- [27] Mitchell, T. (1997). *Machine Learning*. New York: McGraw-Hill. p89.
- [28] Basener, William F., Eric Nance, and John Kerekes. "The target implant method for predicting target difficulty and detector performance in hyperspectral imagery." In *Algorithms and Technologies for Multispectral, Hyperspectral, and Ultraspectral Imagery XVII*, vol. 8048, p. 80481H. International Society for Optics and Photonics, 2011.